RAPID COMMUNICATIONS

PHYSICAL REVIEW B VOLUME 48, NUMBER 22 1 DECEMBER 1993-II

Linear temperature dependence of the transverse electrical resistivity of organic metals arising from electron-electron umklapp scattering

I. Batistić and B. Korin-Hamzić
Institute of Physics of the University, Bijenička c. 46, 41000 Zagreb, Croatia

J. R. Cooper
Institute of Physics of the University, Bijenička c. 46, 41000 Zagreb, Croatia
and IRC in Superconductivity, University of Cambridge, Madingley Road, Cambridge CB3 0HE, United Kingdom

(Received 28 June 1993)

We have calculated the electron-electron scattering contribution to the electrical resistivity ($\rho_\perp$) in the two transverse directions for an anisotropic tight-binding cosine band. This type of band structure is thought to apply to organic metals such as the Bechgaard salts. Simple expressions for $\rho_\perp$ were obtained using the standard variational method. In all cases we found $\rho_\perp = \alpha T + \beta T^2$. For the b direction $\alpha \sim t_b^{-2}$ and $\beta \sim t_b^{-3}$, and for the c axis $\alpha \sim t_c^{-2}$ while the expression for β is more complicated. The above formulas are compared with experimental data and the effective Coulomb interaction for the Bechgaard salts is found to be $U \simeq 0.64$ eV.

Most organic metals are composed of large planar molecules stacked face to face in chains. The anisotropy of the π orbitals leads to good electronic overlap along the chains and much weaker overlap in the transverse directions. For example, the electron spectrum of a large family of organic conductors, the Bechgaard salts, can be approximately represented by a simple tight-binding formula with effective transfer integrals, $t_\parallel$, t_b, and t_c, corresponding to the high, intermediate, and low conductivity directions, respectively. For the Bechgaard salts typical values of $t_\parallel$, t_b, and t_c are 347, 23,[1] and 0.1–1 meV,[2,3] respectively. If the weak dimerization along the chains is neglected, one deals with a quarter filled hole band whose Fermi energy $E_F \approx 2t_\parallel(1-0.707) \simeq 203$ meV. The Fermi surface (FS) is open in both transverse directions. Typical values of the lattice constants, e.g., for $(\mathrm{TMTSF})_2\mathrm{ClO}_4$ are a=3.62, b=7.678, and c=13.275 Å.[4]

Measurements of the intrinsic temperature (T) dependences of the resistivity for the three perpendicular directions ρ_a, $\rho_{b'}$, and ρ_{c^*} are often complicated or rendered invalid by the occurrence of sudden irreversible jumps in resistance-temperature plots which are caused by microcracks in these small fragile crystals. This is especially serious for measurements of $\rho_a(T)$. However, early work on $(\mathrm{TMTSF})_2\mathrm{PF}_6$ using either dc or 35 GHz (where cracks are less important) showed that $\rho_a(T) \sim T^2$ (30–300 K),[5] $\rho_{b'}(T) \sim T^1$ (30-300 K),[5,6] and $\rho_{c^*}(T) \sim T^2$ (20–70 K).[6]

In several cases these measurements have been confirmed by other groups using dc, e.g., $\rho_a(T)$ of $(\mathrm{TMTSF})_2\mathrm{ClO}_4$,[7] $\rho_{c^*}(T)$ of $(\mathrm{TMTSF})_2\mathrm{ClO}_4$ and $(\mathrm{TMTSF})_2\mathrm{PF}_6$,[2] and $\rho_{b'}(T)$ of $(\mathrm{TMTSF})_2\mathrm{NO}_3$.[8] Furthermore we noticed some time ago that for $(\mathrm{TMTSF})_2\mathrm{ClO}_4$ the T^2 behavior of ρ_{c^*} changes over to a linear dependence below 10 K.[2]

In this paper we show that the T^1 behavior in $\rho_b(T)$ and ρ_{c^*} can arise from electron-electron scattering when $k_BT \leq t_b$ or t_c. Until now it has generally been found that electron-electron scattering gives rise to a T^2 law. The exceptions are either for the special case of a one-dimensional half-filled band[9] or for a model which may apply to the organic conductor TTF-TCNQ where there are two types of chains and two partially filled one-dimensional bands crossing at the Fermi-level.[10] The basic physical picture is sketched below followed by the results of numerical calculations. These enable the effective electron-electron Coulomb interaction to be estimated from the linear terms in ρ_{c^*} of $(\mathrm{TMTSF})_2\mathrm{ClO}_4$.

As explained in various textbooks the T^2 law arises simply from the need to conserve both energy and crystal momentum in electron-electron collisions. For a spherical [or general three-dimensional (3D)] Fermi surface and a given initial state, the energies of the other initial state and one of the final states can vary independently by $\approx \pm 2k_BT$, and it is still possible to conserve energy E and momentum $\mathbf{k}$. Thus the number of allowed scattering processes increases as T^2 leading to T^2 behavior of $\rho(T)$. Such behavior is generally obtained when the integrals over $\mathbf{k}$ and the integrals over E can be factorized out.[11] For a half-filled one-dimensional band sketched in Fig. 1(a) the origin of the linear T^1 behavior arising from electron-electron umklapp scattering can be seen as follows. Without loss of generality one initial state can be considered to be at the Fermi level ($E_1 = E_F$). Then, in order to conserve E and $\mathbf{k}$, the other initial state (2) must also have the same energy ($E_2 = E_F$). If this is not the case then simultaneous conservation of E and $\mathbf{k}$ is impossible. The two final states (3, 4) must then be symmetrically disposed about E_F as sketched in Fig. 1(a), and integration over E_3 leads to $\rho_a \sim T^1$. The main point of this paper is that similar constraint applies for the *transverse* resistivity of a tight-binding cosine band with arbitrary band filling. For example, for the (transverse) umklapp scattering process sketched in Fig. 1(b) only one of the energies can be varied independently—leading to $\rho_\perp \sim T^1$. In contrast for the umklapp process shown in Fig. 1(c) where all four states are on the same side of the Fermi surface, a T^2 law is obtained because E_2 and E_3 can be varied independently and still satisfy

E and $\mathbf{k}$ conservation. These two points can be shown by simple geometry and are confirmed by detailed calculations outlined below.

According to the standard variational method for the solution of the Boltzmann transport equation[12] the electrical resistivity is given by

$$\rho = \frac{(k_B T)^{-1}\mathcal{I}}{\mathcal{V}\left|\int \frac{d\mathbf{k}}{(2\pi)^3}\, e\, v_{\mathbf{k}}\, \Phi_{\mathbf{k}}\, \frac{\partial f_{\mathbf{k}}}{\partial E_{\mathbf{k}}}\right|^2}. \tag{1}$$

Here $\mathcal{V}$ is the volume of the system, $f_{\mathbf{k}}$ is the Fermi distribution function, $E_{\mathbf{k}}$ is the electron energy, $\mathbf{v}_{\mathbf{k}} = \hbar^{-1}\boldsymbol{\partial}_{\mathbf{k}} E_{\mathbf{k}}$ is the electron velocity, and $\Phi_{\mathbf{k}}$ is a variational trial function. As usual, we assume that the trial function $\Phi_{\mathbf{k}}$ is proportional to the electron velocity in the direction of applied electric field $\boldsymbol{\mathcal{E}}$, $\Phi_{\mathbf{k}} = \boldsymbol{\mathcal{E}} \cdot \mathbf{v}_{\mathbf{k}}$. $\mathcal{I}$ represents the entropy production integral arising from electron scattering processes.[12] Here we consider only electron-electron scattering processes and thus

$$\mathcal{I} = \frac{1}{4(2\pi)^{12}} \int d\mathbf{k}d\mathbf{k}'d\mathbf{k}_1 d\mathbf{k}_1' \;\; [\Phi_{\mathbf{k}} + \Phi_{\mathbf{k}'} - \Phi_{\mathbf{k}_1} - \Phi_{\mathbf{k}_1'}]^2 |V_{\mathbf{k}\mathbf{k}';\mathbf{k}_1\mathbf{k}_1'}|^2$$
$$\times \frac{2\pi}{\hbar}\delta(E_{\mathbf{k}} + E_{\mathbf{k}'} - E_{\mathbf{k}_1} - E_{\mathbf{k}_1'}) f_{\mathbf{k}} f_{\mathbf{k}'} (1 - f_{\mathbf{k}_1})(1 - f_{\mathbf{k}_1'}). \tag{2}$$

$V_{\mathbf{k}\mathbf{k}';\mathbf{k}_1\mathbf{k}_1'}$ is the matrix element of the Coulomb interaction between the two initial states $\mathbf{k}$, $\mathbf{k}'$ and two final states $\mathbf{k}_1$, $\mathbf{k}_1'$,

$$|V_{\mathbf{k}\mathbf{k}';\mathbf{k}_1\mathbf{k}_1'}|^2 \simeq \mathcal{V} {V^{(N)}_{\mathbf{k}\mathbf{k}';\mathbf{k}_1\mathbf{k}_1'}}^{2} (2\pi)^3 \delta(\mathbf{k} + \mathbf{k}' - \mathbf{k}_1 - \mathbf{k}_1') + \mathcal{V} \sum_{\mathbf{G}\neq 0} {V^{(U)}_{\mathbf{k}\mathbf{k}';\mathbf{k}_1\mathbf{k}_1'}}^{2} (\mathbf{G}) (2\pi)^3 \delta(\mathbf{k} + \mathbf{k}' - \mathbf{k}_1 - \mathbf{k}_1' - \mathbf{G}). \tag{3}$$

The first part of Eq. (3) corresponds to normal electron-electron scattering processes (N processes) and the second term corresponds to umklapp processes (U processes). Usually umklapp processes give the dominant electron-electron contribution to the resistivity except when the effective mass varies strongly over the FS. On the other hand umklapp matrix elements are usually smaller, $|V^{(N)}| \gg |V^{(U)}|$. However, in these materials the Thomas-Fermi wave vector, $k_{\mathrm{TF}}^2 = 4\pi\, e^2 N_F \simeq 4e^2/(abc\; t_{\|}) > (2\pi)^2/bc$, is of the same order as the reciprocal lattice vectors. Thus the effective (screened) Coulomb interactions for U and N processes are comparable, $|V^{(U)}(\mathbf{G}_\perp)| \approx |V^{(N)}|$ for the first few umklapp wave vectors $\mathbf{G}_\perp$, perpendicular to the chain which are important for the transverse resistivity. Likewise, we can neglect the $\mathbf{k}_\perp$ dependence of the Coulomb matrix elements $V^{(N)}$ and $V^{(U)}$. The k_x dependence will be approximated in the usual way by introducing two interaction terms corresponding to the Coulomb interaction with small and large ($\approx\; 2k_F$) momentum transfers:

$$V^{(U/N)}_{\mathbf{k}\mathbf{k}';\mathbf{k}_1\mathbf{k}_1'} = \begin{cases} \mathcal{V}_0 U_1 & \text{if } |k_x + k'_x - k_{1x} - k'_{1x} - 2k_F| \ll k_F \\ \mathcal{V}_0 U_2 & \text{if } |k_x + k'_x - k_{1x} - k'_{1x}| \ll k_F, \end{cases} \tag{4}$$

where $\mathcal{V}_0 = abc$ is the unit cell volume. We also linearize the electron energy spectrum around the Fermi wave vectors, $E_{\mathbf{k}} = E_F \pm \hbar\, v_F \left[k_x \mp k_{FS}^{(\pm)}(\mathbf{q}_\perp)\right]$, where $E_F = -2t_{\|}\cos(k_F a)$ is the Fermi energy, and k_F and $v_F = 2\hbar^{-1} a\; t_{\|}\sin(k_F a)$ are the average values of the Fermi wave vector and Fermi velocity in the x direction. The Fermi surface (FS) can then be described by $k_{\mathrm{FS}}^{(\pm)}(\mathbf{q}_\perp) = k_F \pm (\hbar v_F)^{-1}[2t_b\cos(k_y b) + 2t_c\cos(k_z c)]$.

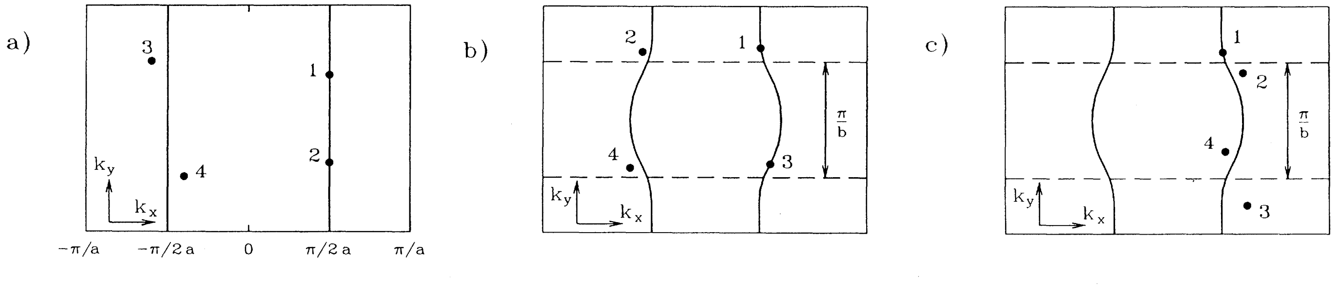

FIG. 1. (a) Electron-electron umklapp scattering for a 1D half-filled band. As explained in the text, in order to conserve energy and momentum the initial states 1 and 2 and the final states 3 and 4 must be symmetrically disposed around E_F. So if $E_1 = E_F$ as drawn, then $E_2 = E_F$, $E_3 + E_4 = 2\; E_F$, and $\rho_{\|} \sim T^1$. (b) Electron-electron umklapp scattering for the transverse resistivity of an anisotropic quasi-one-dimensional "cosine" band. If the initial states 1 and 2 are on opposite sides of the FS only one of the energies, e.g., E_2, can vary independently and hence $\rho_\perp \sim T^1$. (c) If both initial states are on the same side of the FS then E_2 and E_3 can vary independently leading to $\rho_\perp \sim T^2$.

Because of momentum conservation only two types of scattering processes give a finite contribution to the entropy integral $\mathcal{I}$ when the band is not half filled. In case A the initial states are on the opposite sides of the FS [Fig. 1(b)] and in case B all states are on the same side of the FS [Fig. 1(c)]. These two cases will be considered separately.

Case (A). First we consider the resistivity for the b direction. The entropy integral $\mathcal{I}$ can be factorized into three four-dimensional integrals, one for each direction in $\mathbf{k}$ space:

$$\begin{aligned}\mathcal{I}_i \simeq \mathcal{E}_b^2(2\pi)^{-8}\hbar^{-3}(t_b b\mathcal{V}_0 U_i)^2 &\int d^4k_z \sum_{G_z} \delta(k_z + k'_z - k_{1z} - k_1{}'_z - G_z) \\ &\times \int d^4k_y \sum_{G_y} \Big(\sin(bk_y) + \sin(bk'_y) - \sin(bk_{1y}) - \sin(bk_1{}'_y)\Big)^2 \, \delta(k_y + k'_y - k_{1y} - k_1{}'_y - G_y) \\ &\times \int d^4k_x \, \delta(\tilde{k}_x + \tilde{k}'_x - \tilde{k}_{1x} - \tilde{k_1}'_x) \, \delta\Big(\hbar \, v_F(\tilde{k}_x - \tilde{k}'_x - \tilde{k}_{1x} + \tilde{k_1}'_x)\Big) \, ff'(1-f_1)(1-f'_1), \end{aligned} \tag{5}$$

where $\tilde{k}_x = k_x \mp k_F$ denotes the electron momentum measured with respect to the Fermi wave vector. The k_z and k_y integrals yield constant factors, $(2\pi/c)^3$ and $2(2\pi/b)^3$, respectively. The third k_x set of integrals provide a temperature dependent term, $(k_BT)^2/2(\hbar v_F)^3$. Substituting back into Eq. (1) we obtain a linear (l) contribution to ρ_b:

$$\rho_b^{(l)} = \frac{\hbar}{e^2} \frac{ac(U_{1\|}^2 + U_{2\|}^2 + U_{1\perp}^2 + U_{2\perp}^2)k_BT}{16\sin(ak_F)bt_\| t_b^2}, \tag{6}$$

where $U_{i\|}$ and $U_{i\perp}$ are Hubbard-like electron-electron interactions, as defined by Eq. (4), for electrons with parallel and antiparallel spins, respectively.

The calculations for the c direction are completely similar and the result can be obtained from Eq. (6) by the substitutions $b \leftrightarrow c$ and $t_b \leftrightarrow t_c$.

Case (B). For an electric field applied along the b direction, the entropy production integral $\mathcal{I}$ can again be factorized into three terms corresponding to different space directions:

$$\begin{aligned}\mathcal{I}_i \simeq \mathcal{E}_b^2(2\pi)^{-8}\hbar^{-3}(t_b b\mathcal{V}_0 U_i)^2 &\int d^4k_z \sum_{G_z} \delta(k_z + k'_z - k_{1z} - k_1{}'_z - G_z) \\ \times \int d^4k_y \sum_{G_y} &\Big(\sin(bk_y) + \sin(bk'_y) - \sin(bk_{1y}) - \sin(bk_1{}'_y)\Big)^2 \, \delta\Big(-2t_b[\cos(bk_y) + \cos(bk'_y) - \cos(bk_{1y}) \\ - \cos(bk_1{}'_y)]\Big) \, &\delta(k_y + k'_y - k_{1y} - k_1{}'_y - G_y) \int d^4k_x \, \delta(\tilde{k}_x + \tilde{k}'_x - \tilde{k}_{1x} - \tilde{k_1}'_x) \; ff'(1-f_1)(1-f'_1). \end{aligned} \tag{7}$$

The k_z and k_y integrals yield constant factors, $(2\pi/c)^3$ and $64/t_b b^3$, respectively, while the k_x integral is equal to $(2\pi^2/3)(k_BT/\hbar v_F)^3$. The final result is a quadratic (q) term:

$$\rho_b^{(q)} = \frac{\hbar}{e^2} \frac{ac(U_{2\|}^2 - U_{2\perp}^2)(k_BT)^2}{6\pi \sin(ak_F)bt_\| t_b^3}, \tag{8}$$

Unlike the previous cases, the corresponding calculation for the c direction is much more complicated because the k_z and k_y integrations cannot be decoupled:

$$\begin{aligned}\mathcal{I}_i \simeq \mathcal{E}_c^2(2\pi)^{-8}\hbar^{-3}(t_c c\mathcal{V}_0 U_i)^2 &\int d^4k_x \, \delta(\tilde{k}_x + \tilde{k}'_x - \tilde{k}_{1x} - \tilde{k_1}'_x) \; ff'(1-f_1)(1-f'_1) \\ &\times \int d^4k_z \sum_{G_z} \delta(k_z + k'_z - k_{1z} - k_1{}'_z - G_z) \, \Big(\sin(ck_z) + \sin(ck'_z) - \sin(ck_{1z}) - \sin(ck_1{}'_z)\Big)^2 \\ &\times \int d^4k_y \sum_{G_y} \delta(k_y + k'_y - k_{1y} - k_1{}'_y - G_y) \, \delta\Big(-2t_b \cdot [\cos(bk_y) + \cos(bk'_y) \\ &- \cos(bk_{1y}) - \cos(bk_1{}'_y)] - 2t_c[\cos(ck_z) + \cos(ck'_z) - \cos(ck_{1z}) - \cos(ck_1{}'_z)]\Big). \end{aligned} \tag{9}$$

We notice that the k_y part of the integration diverges logarithmically for small t_c. Therefore we have to keep the t_c part of the electron spectrum within the δ function as a cutoff. The calculations can be done approximately if $t_c \ll t_b$. Eventually we obtain that the T^2 part of ρ_c is

$$\rho_c^{(q)} = \frac{\hbar}{e^2} \frac{ab(U_{2\|}^2 + U_{2\perp}^2)F(t_c/t_b)(k_BT)^2}{48\pi \sin(ak_F)ct_\| t_b t_c^2}, \tag{10}$$

where $F(t_c/t_b) = 6.1 - 3.6\ln(t_c/t_b) + 0.5\ln^2(t_c/t_b)$.

The above equations for ρ_b and ρ_c can be compared with experimental data for the Bechgaard salts. We do not discuss ρ_b here because although experiments clearly show T^1 behavior there is still some doubt about the magnitudes. Furthermore, some numerical factors may be altered because of the monoclinic structure. Usually band formulas are only valid when the mean free paths are larger than the lattice constants, which means that Eqs. (6), (8), and (??) may only apply for $\rho_b \leq 0.007\ \Omega$ cm (if $t_{\|}/t_b = 17$) and $\rho_c \leq 0.03\ \Omega\,\mathrm{cm}$ (if $t_{\|}/t_c = 250$).

Figure 2 shows experimental data for $\rho_{c^*}(T)$ of $(\mathrm{TMTSF})_2\mathrm{ClO}_4$ in the slowly cooled (relaxed) state where the ClO_4 anions are well ordered. A second-order polynomial fit enables possible linear and quadratic contributions to be estimated. Similar data were obtained for the two other crystals studied. The magnitude of the linear term corresponds to a resistivity of 0.035 Ω cm at 12 K [taking $\rho_{c^*}(300\ \mathrm{K}) = 6\ \Omega\,\mathrm{cm}$ (Ref. 2)]. An upper limit to the phonon contribution to $\rho_c(T)$ is given by scaling $\rho_a(T)$(Ref. 14) by $\overline{v_a^2}/\overline{v_c^2}$; at 12 K it is a factor of 5 lower than the latter value. The value of t_c determined from the low-temperature magnetoresistance[2,13] is $1\pm\ 0.2$ meV. Together with the other parameters given previously and the appropriate form of Eq. (6) for ρ_c, we find an average value $\overline{U} \simeq 0.64$ eV.

Using the above value of $\overline{U}$ we can estimate the expected T^2 term in ρ_{c^*} of $(\mathrm{TMTSF})_2\mathrm{ClO}_4$ from Eq. (10). The theoretical value corresponds to a resistivity of $2.5\times10^{-3}\ \Omega$ cm at 12 K, which is a factor of 10 lower than the experimental value obtained from the fits shown in Fig. 2. So the present analysis cannot account for the crossover in ρ_{c^*} from T^1 to T^2 observed near 15 K. The doubling of the b lattice parameter associated with the anion ordering transition in $(\mathrm{TMTSF})_2\mathrm{ClO}_4$ at 24 K makes the value of t_b somewhat uncertain, but this cannot be responsible for such a large discrepancy because the T^2 term in ρ_{c^*} only changes by $\sim 30\%$ above 24 K.[2,13] The possible reasons for this discrepancy are either the monoclinic symmetry or the short mean free path. However, in the latter case one might expect unusual effects in magnetoresistance in this temperature range which were not observed.[2]

Although we have not calculated $\rho_a(T)$ there is evidence for a T^1 dependence from $\sim$ 20 K down to the superconducting transition.[15] Further work is needed to see whether this is caused by electron-electron scattering and whether it can account for hot spots[6] or hot strips[16] which may be responsible for the anomalous magnetoresistance and magic angles, respectively.

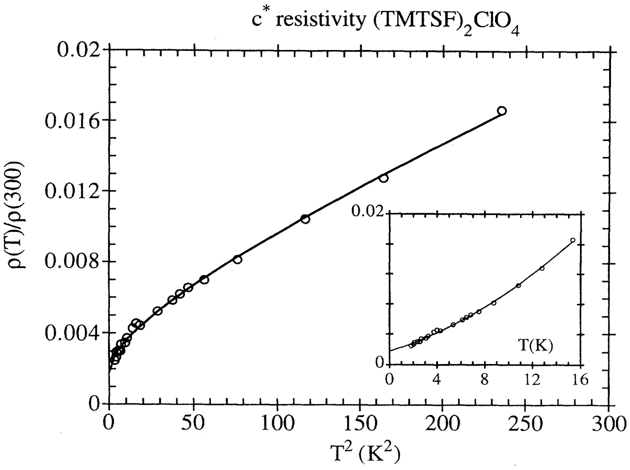

FIG. 2. Normalized resistivity versus T^2 for a representative crystal of $(\mathrm{TMTSF})_2\mathrm{ClO}_4$ in the low conductivity c^* direction. The inset shows the data on a linear temperature scale. In both cases the solid line is a polynomial fit: $R/R_{300} = 0.001\,79 + 7.21\times10^{-3}(T/15) + 7.0\times10^{-3}(T/15)^2$, i.e., the T^2 term becomes dominant above $k_BT \approx 1$ meV $\approx t_c$.

Finally the present analysis implies that measurements of the pressure dependence of ρ_c, in combination with a determination of t_c from magnetoresistance,[2] could be used to follow the pressure dependence of the effective Coulomb interaction $\overline{U}$ (caused by changes in screening) and its connection (if any) with the suppression of the superconducting transition temperature.

On the theoretical side another question is whether the relatively large low-temperature value of $\overline{U}$ ($\approx$ 0.6 eV) obtained here is at all consistent with, for example, the low spin density wave ordering temperature of $(\mathrm{TMTSF})_2\mathrm{PF}_6$ (12 K). Perhaps the answer to this lies in the anomalous screening effects and the momentum dependence of the Coulomb interaction in these highly anisotropic compounds.

We have benefited from useful discussions with S. Barišić, A. Bjeliš, L. Forró, D. Jérome, and S. Tomić.

---

[1] P.M. Grant, J. Phys. (Paris) Colloq. **44**, C3-847 (1983). See also P.M. Grant, Phys. Rev. B **26**, 6888 (1982).

[2] J.R. Cooper, L. Forró, B. Korin-Hamzić, K. Bechgaard, and A. Moradpour, Phys. Rev. B **33**, 6810 (1986).

[3] P.M. Grant, J. Phys. (Paris) Colloq. **44**, C3-1121 (1983).

[4] K. Bechgaard, K. Carneiro, F.B. Rasmussen, M. Olsen, G. Rindorf, C.S. Jacobsen, H.J. Pedersen, and J.C. Scott, J. Am. Chem. Soc. **103**, 2440 (1981). The quoted value of a is the distance between TMTSF molecules in the chain direction and is 1/2 of the lattice parameter. The weak dimerization in the a direction has been neglected.

[5] K. Bechgaard, C.S. Jacobsen, K. Mortensen, H.J. Pedersen, and N. Thorup, Solid State Commun. **33**, 1119 (1980).

[6] C.S. Jacobsen, K. Mortensen, M. Weger, and K. Bechgaard, Solid State Commun. **38**, 423 (1981).

[7] K. Murata, T. Ukachi, H. Anzai, G. Saito, K. Kajimura, and T. Ishiguro, J. Phys. Soc. Jpn. **51**, 1817 (1982).

[8] S. Tomić *et al.* (unpublished).

[9] L.P. Gor'kov and I.E. Dzyaloshinsky, Pis'ma Zh. Eksp. Teor. Fiz. **18**, 686 (1973) [JETP Lett. **18**, 401 (1973)].

[10] G.J. Morgan and J.R. Cooper, J. Phys. F **11**, 2091 (1981).

[11] C. Potter and G.J. Morgan, J. Phys. F **9**, 493 (1979).

[12] J.M. Ziman, *Electrons and Phonons* (Oxford University Press, London, 1960).

[13] B. Korin-Hamzić, L. Forró, J.R. Cooper, and K. Bechgaard, Phys. Rev. B **38**, 11177 (1988).

[14] M. Weger, M. Kaveh, and H. Gutfreund, Solid State Commun. **37**, 421 (1981); E.M. Conwell and C.S. Jacobsen, *ibid.* **40**, 203 (1981).

[15] D. Jérome and H.J. Schulz, Adv. Phys. **31**, 299 (1982).

[16] P.M. Chaikin, Phys. Rev. Lett. **69**, 2831 (1992).